Cell, Vol. 97, 471–480, May 14, 1999, Copyright ©1999 by Cell Press

Structure of the Enabled/VASP Homology 1 Domain–Peptide Complex: A Key Component in the Spatial Control of Actin Assembly

Kenneth E. Prehoda, Do J. Lee, and Wendell A. Lim*
Departments of Cellular and Molecular Pharmacology and Biochemistry and Biophysics
University of California
San Francisco, California 94143

Summary

The Enabled/VASP homology 1 (EVH1; also called WH1) domain is an interaction module found in several proteins implicated in actin-based cell motility. EVH1 domains bind the consensus proline-rich motif FPPPP and are required for targeting the actin assembly machinery to sites of cytoskeletal remodeling. The crystal structure of the mammalian Enabled (Mena) EVH1 domain complexed with a peptide ligand reveals a mechanism of recognition distinct from that used by other proline-binding modules. The EVH1 domain fold is unexpectedly similar to that of the pleckstrin homology domain, a membrane localization module. This finding demonstrates the functional plasticity of the pleckstrin homology fold as a binding scaffold and suggests that membrane association may play an auxiliary role in EVH1 targeting.

Introduction

Many cells have the ability to move or alter their shape in response to external signals. Such movements, observed in an extending axon, a migrating neutrophil, or an invasive tumor cell, are mediated by remodeling of the actin cytoskeleton (Mitchison and Cramer, 1996). A primary requirement for directional movement is the establishment of cell polarity—actin polymerization must be targeted to the cell's leading edge, where it is thought to provide a forward mechanical force for membrane protrusion and adhesion. Thus, a fundamental question in cell motility is how external signals are used to establish sites of actin polymerization.

A family of adapter proteins, including Enabled (Ena), vasodilator-stimulated phosphoprotein (VASP), and Wiskott-Aldrich syndrome protein (WASP), has recently been implicated in the spatial control of actin assembly. Current models suggest that these proteins localize to potential leading edge sites via interactions with upstream signaling proteins. Subsequently, they are thought to act as scaffolds to recruit or activate downstream components of the actin assembly machinery (Pollard, 1995; Machesky, 1997; Beckerle, 1998) (Figure 1A).

Several lines of evidence support a model in which Ena/VASP/WASP proteins couple signaling pathways to actin polymerization. First, these proteins are required for diverse actin-based processes, ranging from budding and cytokinesis in yeast (Li, 1997) to neutrophil chemotaxis (Symons et al., 1996) and axon guidance in mammals (Lanier et al., 1999). Second, these proteins specifically localize to sites of actin dynamics such as the leading edge of motile cells and focal adhesions, sites of cellular communication with the extracellular matrix (Gertler et al., 1996; Symons et al., 1996). Third, overexpression of certain isoforms of mammalian Enabled (Mena) or WASP yields spontaneous actin microspike formation (Gertler et al., 1996; Symons et al., 1996). Finally, these proteins share an overall structural organization consistent with an adapter function: they have regions that interact with upstream signaling proteins and regions that interact with components of the actin assembly machinery (Gertler et al., 1996; Symons et al., 1996; Machesky and Insall, 1998). Proteins recruited by the Ena/VASP/WASP family include profilin and the Arp2/3 complex, which are thought to directly promote actin filament elongation and nucleation (Reinhard et al., 1995; Machesky and Insall, 1998) (Figure 1B).

Proper site selection by Ena/VASP/WASP proteins requires a novel protein interaction domain referred to as the Enabled VASP homology 1 (EVH1) or the WASP homology 1 (WH1) domain (Gertler et al., 1996; Symons et al., 1996) (Figure 1B). This domain is found at the N terminus of all family members. Although some reports have treated the domains from Ena and WASP as distinct, recent multisequence alignments indicate that they are members of the same family (Ponting and Phillips, 1997). The EVH1 domain from Mena can independently localize to sites of actin remodeling (Gertler et al., 1996).

EVH1 domain localization occurs through binding to proline-rich motifs of consensus sequence FPPPP (Niebuhr et al., 1997) (Figure 1C). Such motifs are found in several proteins involved in transmitting external signals to the actin cytoskeleton, including the focal adhesion proteins zyxin and vinculin (Niebuhr et al., 1997) and the axon guidance receptors SAX-3/Robo (Kidd et al., 1998; Zallen et al., 1998). Accessibility of these motifs can be regulated by the activation state of the proteins (Huttelmaier et al., 1998).

EVH1 domain interactions are also required to recruit the actin assembly machinery to the surface of the motile intracellular pathogen *Listeria monocytogenes* (Chakraborty et al., 1995; Niebuhr et al., 1997; Laurent et al., 1999). This bacteria uses its surface protein ActA to hijack host cytoskeletal proteins, thereby generating a propulsive actin comet tail that allows the bacteria to move and infect neighboring cells (Tilney and Portnoy, 1989; Theriot et al., 1994). Multiple EVH1-binding motifs are found in ActA (Figure 1C) (Chakraborty et al., 1995; Niebuhr et al., 1997). These motifs recruit Mena and VASP to the base of the *Listeria* comet tail (Gertler et al., 1996) and are required for high speed motility (Smith et al., 1996). Furthermore, injection of EVH1-binding peptides into cells is sufficient to block proper localization of Mena or VASP and to inhibit *Listeria* movement (Southwick and Purich, 1994; Niebuhr et al., 1997).

*To whom correspondence should be addressed: (e-mail: wlim@itsa.ucsf.edu).

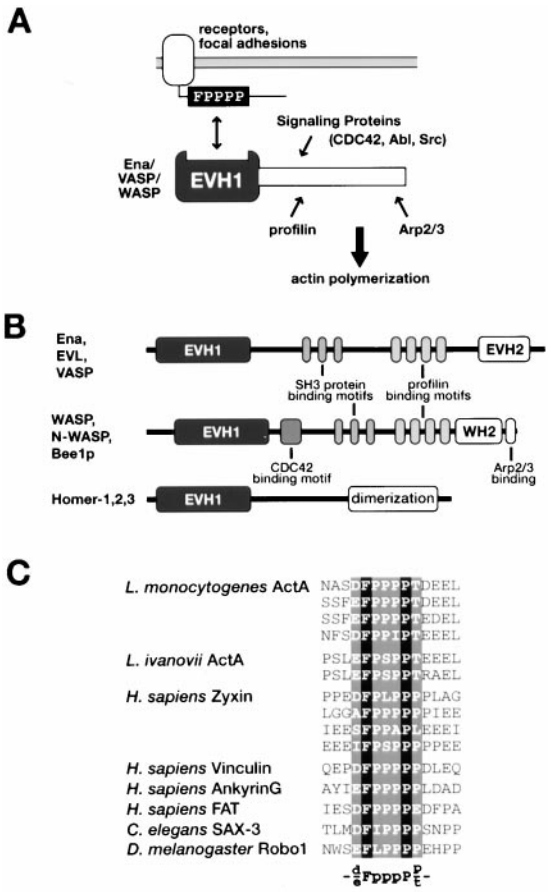

Figure 1. Structure and Function of EVH1 Domain–Containing Proteins

(A) Ena/VASP/WASP proteins spatially regulate actin dynamics. Localization occurs via interactions of the EVH1 domain. Other regions recruit proteins that directly promote actin polymerization (profilin, Arp2/3 complex). Interactions with signaling molecules may modulate these events.

(B) Domain structure of EVH1-containing proteins. The Enabled/VASP and WASP/N-WASP subfamilies are involved in regulation of the actin cytoskeleton and contain motifs that can interact with various signaling proteins (Finan et al., 1996; Gertler et al., 1996; Symons et al., 1996) and actin-binding proteins (Reinhard et al., 1995; Gertler et al., 1996; Machesky and Insall, 1998). The Homer subfamily plays a role in synaptic plasticity (Brakeman et al., 1997).

(C) Alignment of EVH1 binding sequences (Niebuhr et al., 1997), including sequences from the *Listeria* ActA proteins, host cytoskeletal proteins (zyxin, vinculin, ankyrin), and host axon guidance receptors (SAX-3, Robo). Identical residues are highlighted in solid, and conserved ones are shaded. Consensus sequence is shown below.

Interestingly, EVH1 domains are also found in a distinct class of proteins with no known link to the actin cytoskeleton. These proteins belong to the Homer/Vesl family of postsynaptic proteins that are thought to function in synaptic plasticity (Brakeman et al., 1997; Kato et al., 1997). The Homer/Vesl EVH1 domains bind proline-rich motifs found in the metabotropic glutamate receptor (mGluR) and inositol 1,4,5-trisphosphate (IP3) receptor (Tu et al., 1998). These examples may represent an expanded evolutionary use of the EVH1 domain as a localization module.

To understand the structural basis of EVH1 domain localization, we have determined the crystal structure of the EVH1 domain of Mena in complex with a proline-rich peptide derived from ActA to 1.8 Å resolution. The ligand is recognized by a mechanism distinct from that of Src homology 3 (SH3) domains and other previously characterized proline-binding modules. The Mena EVH1 domain fold is unexpectedly similar to that of the pleckstrin homology (PH) domain, a membrane localization module. This structural similarity suggests that EVH1 domains may target leading edge sites during cell movement by interacting with both proteins and membranes.

Results

Biophysical Characterization of the EVH1 Domain–Peptide Interactions

Binding of the Mena EVH1 domain (residues 1–112) to various peptides was characterized by a quantitative fluorescence perturbation assay (Figure 2A). These peptides show a wide range of affinities (Figure 2B). Minimal "core" peptides (Niebuhr et al., 1997) bind with low but measurable affinities ($K_D \geq 400$ μM). Peptides flanked by clusters of C-terminal acidic residues, however, bind with considerably higher affinities ($K_D \geq 5$ μM). Interestingly, the motif from the *Listeria* protein ActA has the highest number of acidic residues and binds with the highest affinity.

We also characterized the peptide binding specificities of EVH1 domains from several different proteins using a qualitative far Western binding assay. EVH1 domains from Mena, WASP, and Homer were tested against an array of putative ligand sequences (Figure 2C). All of the EVH1 domains were found to bind proline-rich peptides but with distinct sequence preferences. Both the Mena and WASP domains bind the ActA peptide with high affinity and in a sequence-specific manner that requires Phe-1. The Mena domain can also bind a related sequence from the human axon guidance receptor, h-Robo1, while the WASP domain does not. The Homer domain shows the greatest differences. It is the only domain that can bind the previously identified motif TPPSPFR found in group 1 metabotropic glutamate receptors (Tu et al., 1998), but it binds only weakly to the ActA peptide. Thus, diverse members of the EVH1 domain family retain the ability to bind distinct proline-rich peptides.

Crystal Structure of the Mena EVH1 Domain–FPPPPT Complex

The Mena EVH1 domain (residues 1–112) was cocrystallized with the ActA-derived peptide Ac-FPPPPT-$CONH_2$. Crystals grew in space group $C222_1$ with one complex per asymmetric unit and diffracted X-rays to 1.8 Å resolution. Experimental phases were determined using multiwavelength anomalous dispersion (MAD) with selenomethionyl-substituted protein (Table 1). The solvent-flattened electron density map was readily interpretable and allowed a model for Mena residues 2–112 to be built. Although the peptide was visible in the experimental map, it was not included until a later stage in the refinement, at which point a model for residues 1–5 was added. Only weak density was observed for Thr-6, the peptide's C-terminal residue. The refined EVH1–peptide

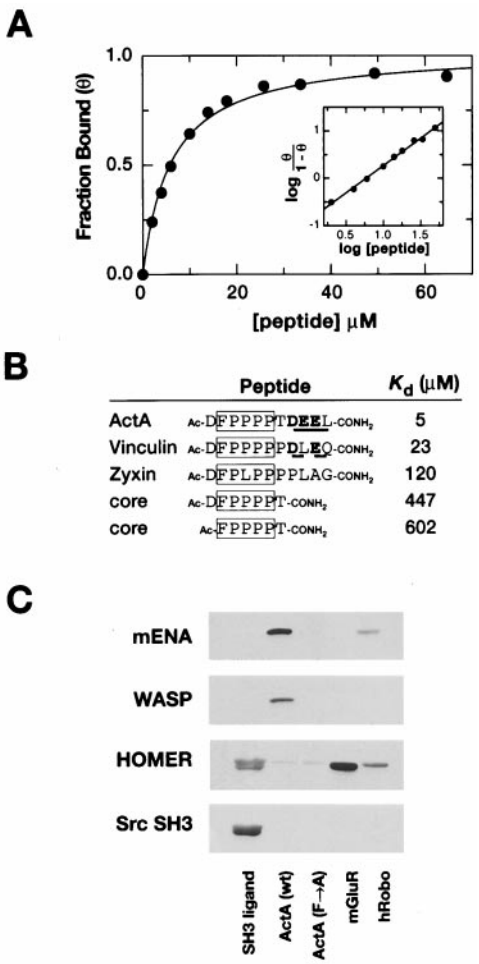

Figure 2. Binding of EVH1 Domains to Proline-Rich Peptides

(A) Binding of ActA peptide (DFPPPPTDEEL) to the Mena EVH1 domain, measured using a fluorescence perturbation assay. Hill cooperativity plot (inset) indicates a 1:1 stoichiometry.

(B) Binding affinities of peptide ligands to Mena EVH1 domain measured by fluorescence perturbation. "Core" indicates conserved sequence found in most EVH1 ligands (boxed). Acidic residues C-terminal to the core are underlined. Standard deviation is ±10%.

(C) Specificity of EVH1 domains detected by far Western overlay assay. Biotinylated fusion proteins containing the EVH1 domains of Mena (1–112), hWASP (1–170), and dHomer (1–112) were used as probes for peptide recogntion. A similar fusion to the Src SH3 domain was used as a control probe. These probes were tested against a series of putative peptides ligands (fused to glutathione S-transferase) blotted onto nitrocellulose. Peptide sequences and their proteins of origin are as follows: SH3 ligand from mSos (gsPVPPPVPPRRgggpgggrsPVPPPVPPRRihr), ActA (gsD**F**PPPPTDEELrla), ActA Phe-to-Ala mutation (gsD**A**PPPRDEELrla), mGluR (gsDLEELVALTPPSPFRD), hRobo (gsTDDLPPPVPPPAIK).

complex has a crystallographic R value of 22.9% and a free R value of 26.8% (Table 1).

The EVH1 domain is composed primarily of two antiparallel β sheets that form a β sandwich (Figure 3A). One end of the β sandwich is capped by a C-terminal α helix. Two concave surfaces are formed by the outside of each β sheet. One of these surfaces (formed by strands 1, 5, 6, and 7) serves as the base of the peptide-binding groove. An interstrand loop (residues 16–23) also contributes to the binding surface.

Alignment of other putative EVH1 sequences, including those of the more distantly related proteins WASP and Homer, shows high conservation of residues that form the hydrophobic core and peptide-binding surface (Figure 3C), indicating that these domains all share a common fold and function.

The Peptide-Binding Interface

The proline-rich core of the peptide ligand binds the Mena EVH1 domain in a polyproline II (PPII) conformation, a left-handed helix with three residues per turn (Figure 4A). The peptide docks at a highly aromatic surface, primarily contacting the triad of EVH1 residues Tyr-16, Trp-23, and Phe-77 (Figure 4B). The complex buries ~300 Å^2 of surface area on the EVH1 domain and ~400 Å^2 on the peptide. The buried backbone carbonyl groups of the peptide, specifically those of Pro-2 and Pro-3, form hydrogen bonds with the side chains of EVH1 residues Gln-79 and Trp-23, respectively. Thus, the EVH1 complex resembles other proline recognition complexes in several fundamental ways: SH3 and WW domains and profilin all use aromatic surfaces to recognize proline-rich peptides in a PPII conformation (Kuriyan and Cowburn, 1997; Mahoney et al., 1997).

Despite these similarities, the overall architecture of the EVH1-binding surface is unique. In the EVH1 domain, the triad of aromatic residues present a concave, V-shaped binding surface (Figure 4A). Consequently, the ligand PPII helix, depicted schematically as a triangular prism, packs against the domain with one of its pointed ends directed into the V-shaped wedge (Figure 4C). In contrast, the binding surfaces of SH3 and WW domains and profilin are relatively flat, with only a series of shallow ridges created by surface-aromatic residues arranged in a parallel fashion. Thus, in complexes involving these domains, a flat face of the ligand PPII helix packs against the domain (Figure 4C) (Feng et al., 1994; Lim et al., 1994; Yu et al., 1994; Mahoney et al., 1997).

Nonproline residues that flank the FPPPP core are recognized through specific interactions. Phe-1, which is a critical specificity element, packs in a pocket just outside the EVH1 aromatic triad. ActA-derived peptides, which are the highest affinity ligands known, all share a cluster of acidic residues C-terminal to the proline core. Although the crystallized peptide does not include these C-terminal residues, the structure indicates that these are likely to interact at a basic surface of the EVH1 domain that is immediately adjacent to the C terminus of the core peptide. Figure 4D illustrates the likely path of the ActA C-terminal acidic residues.

The EVH1 Domain Structurally Resembles PH Domains

The Mena EVH1 domain fold is unexpectedly similar to that of PH domains (Figure 5). PH domains are modules that bind to acidic phospholipids and are thought to mediate membrane localization of the signaling proteins in which they are found (Haslam et al., 1993; Mayer et al., 1993; Bottomley et al., 1998). Although sequence homology between the Mena EVH1 domain and PH domains is extremely low (identity ≤10%, similarity ≤20%), their core structures are quite similar. When the full structure is aligned with known PH domain structures,

Table 1. Data Collection and Refinement Statistics

MAD Phasing				
Energies	No. of Reflections (Total/Unique)	Completeness (%)[a]	Overall I/σ	R_{sym}[a,b]
λ_1 12,400	88,290/17,747	99.1 (91.4)	11.0	9.0 (35.8)
λ_2 12,655	118,018/17,827	99.8 (97.6)	10.8	9.5 (28.9)
λ_3 12,659	121,210/17,696	99.8 (98.5)	11.5	9.9 (22.0)
λ_4 12,800	112,401/18,462	99.7 (97.2)	9.5	9.4 (44.6)
Mean overall figure of merit (30.0–1.8 Å) (centric/acentric) = 0.47/0.66.				

Refinement and Stereochemical Statistics (All Data 30.0–1.8 Å)	
R value	22.9%
Free R value	26.8%
Solvent molecules	26
Average B factors (Å^2)	
Mena 2–112	24.8
Peptide 1–5	32.7
Rms deviations	
Bonds (Å)	0.005
Angles (°)	1.30

[a] Statistics for highest resolution shell (1.9–1.8 Å) in parentheses.
[b] $R_{sym} = \Sigma|I - \langle I\rangle|/\Sigma I$, where I is the integrated intensity of a given reflection.

the α carbon root-mean-square (rms) deviation is large—10–20 Å. However, if only the core β sheets and α helix are considered, the α carbon rms deviation improves to ~2 Å.

Nonetheless, there are several striking differences between the Mena EVH1 domain and PH domains. In the Mena EVH1 domain, the proline-rich peptide ligand binds precisely where, in PH domains, an intramolecular helix/loop normally docks. In PH domains, this large loop or helix insert occurs between β strands 5 and 6 (Figures 5A and 5B) (Macias et al., 1994; Yoon et al., 1994; Ferguson et al., 1995). This insert is missing in the EVH1 domain—a minimal, two-residue β hairpin turn is found in Mena. Phosphotyrosine-binding (PTB) domains, another family of peptide-binding modules that are structurally related to PH domains, also have a loop or helix that packs at this site. In the case of PTB domains, however, this element is inserted between β strands 1 and 2 (Zhou and Fesik, 1995; Zhou et al., 1996; Zhang et al., 1997; Li et al., 1998).

The PH domain fold thus appears to comprise a large but diverse superfamily with at least three phylogenetically distinguishable branches: (1) canonical PH domains, (2) PTB domains, and (3) EVH1 domains (Figure 5C). These different branches of the family use distinct surfaces for peptide or phospholipid ligand recognition (Figure 5A). It is noteworthy that a segment of N-WASP was previously proposed to be a canonical PH domain, based on sequence alignments (Miki et al., 1996). This segment, however, is 50 residues off-register from the EVH1 segment (Ponting and Phillips, 1997), and the very low homology to PH domains appears to be coincidental.

Discussion

EVH1 domains participate in coordinated cell movement by mediating protein localization to the cell's leading edge. Localization by EVH1 domains occurs via binding to proline-rich motifs of the consensus sequence FPPPP, found in various host and pathogen proteins. To understand the molecular basis of EVH1 domain recruitment, we undertook a series of biochemical and structural studies of EVH1 domain interactions with their peptide ligands.

EVH1 Domains Recognize the Helical Character of Their Proline-Rich Ligand

The structure of the EVH1 domain–peptide complex shows that these domains utilize a mechanism of proline motif recognition that primarily focuses on the conformational properties of the ligand rather than the specific identity of residues arrayed along the ligand peptide chain. This mechanism distinguishes EVH1 domains from other proline motif–binding modules, including SH3 and WW domains and profilin, and can explain some of the experimentally observed differences in ligand sequence requirements.

The EVH1 peptide-binding site is concave, setting it apart from the relatively flat surfaces utilized by other proline-rich binding modules (Figure 4). This architecture leads to differences in sequence requirements. Because the SH3 peptide-binding site is essentially flat, it primarily recognizes one surface presented by the ligand PPII helix and does not directly recognize the overall shape of the helix (Feng et al., 1994; Lim et al., 1994; Nguyen et al., 1998). Consequently, for SH3 domains, the precise stereochemical properties of the side chains arrayed on the single contacting surface of the PPII helix are critical for recognition. SH3 ligands, therefore, absolutely require two prolines arrayed in the motif PxxP. At these positions, the unique δ carbon atoms of the proline side chains form a critical part of the recognition interface (Nguyen et al., 1998). Replacement of these two positions with any residue other than proline, all of which lack an N-substituted δ carbon, disrupts recognition. Profilin and WW domain complexes display similar proline-rich peptide recognition mechanisms (Macias et al., 1996; Mahoney et al., 1997).

In contrast, because the EVH1-binding groove is wedge shaped, this domain primarily recognizes the overall helical conformation of the PPII ligand. The

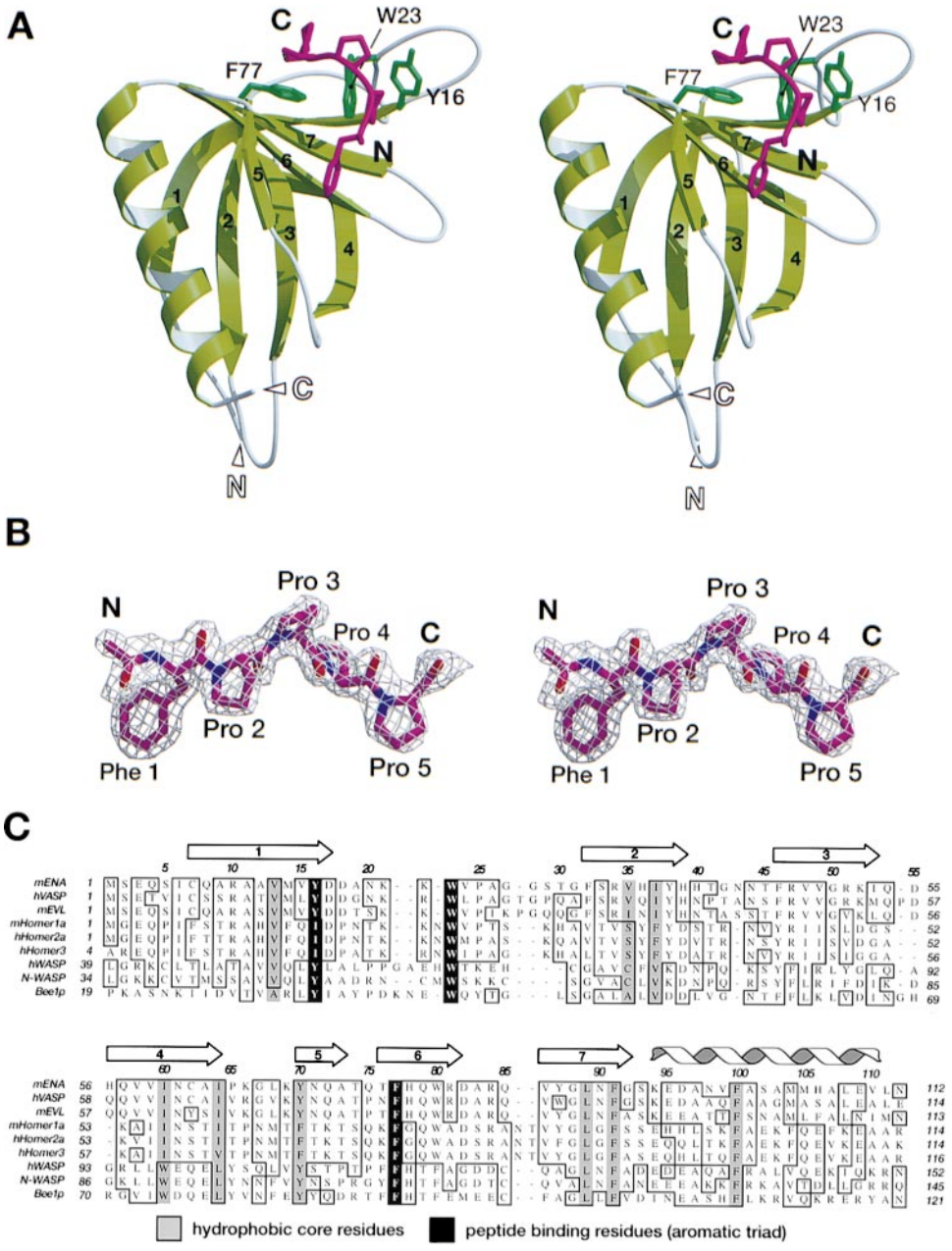

Figure 3. Structure of the Mena EVH1 Domain–Peptide Complex

(A) Stereo ribbon diagram of the Mena EVH1 domain (green) complexed to a core peptide ligand (magenta). Triad of conserved aromatic residues in Mena that make up the binding pocket are also shown. β strands of the domain are numbered.

(B) Electron density of the FPPPP peptide (stereo). Density is from a simulated annealing $2F_o-F_c$ omit map, contoured at 1σ. (A) and (B) were generated with MOLSCRIPT and RASTER3D.

(C) Alignment of EVH1 domains. Sequence numbers for the Mena EVH1 domain shown above. Key positions in the Mena EVH1 domain are highlighted (hydrophobic core, shaded; peptide-binding surface, solid). Amino acid identities are shown in bold, and similarities are boxed. Secondary structure elements in the Mena domain are shown above the sequences.

EVH1-binding surface more closely mirrors the 3-fold helical screw axis of the PPII helix, resembling a matching screw hole. Thus, prolines may be preferred in EVH1 ligands because the PPII conformation is sterically favored by stretches of multiple prolines. This mechanism of binding explains the less restrictive sequence requirements observed for EVH1 domains: proline is strongly preferred but not required at most of the ligand positions (Niebuhr et al., 1997) (Figure 1B). These requirements are consistent with a more indirect conformational role of the peptide prolines—stabilization of the PPII conformation—as opposed to more direct recognition of the proline side chain, as observed in SH3 domains.

Peptide Binding Specificity of EVH1 Domains

Although EVH1 domains recognize the general features of a proline-rich core, they do not bind all proline-rich sequences. For example, most EVH1 domains do not

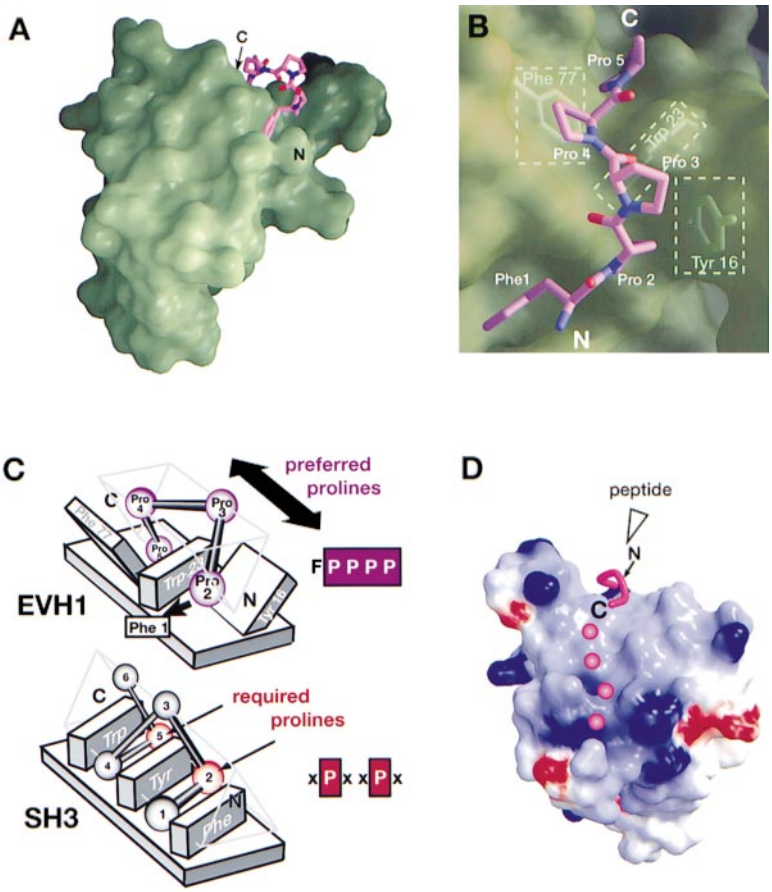

Figure 4. Mechanism of Proline-Rich Peptide Recognition by EVH1 Domains

(A) The peptide ligand (magenta) adopts a PPII-helical conformation and docks into a V-shaped groove on the domain surface (green). The orientation shown is approximately the same as that shown in Figure 3A.

(B) Close-up bird's-eye view of peptide ligand docked against the conserved EVH1 domain aromatic triad (green side chains). PPII-helical axis of the ligand is oriented vertically.

(C) Schematic comparison of EVH1 complex (same orientation as in [A]) and SH3 complex. Both domains use a series of aromatic side chains (planar protrusions) for recognition, but their different arrangement caused the PPII-helical ligand (triangular prism) to dock in different orientations. SH3 recognition focuses on one surface of the PPII helix and therefore absolutely requires prolines at sites labeled 2 and 5. EVH1 recognition focuses more on the overall shape of the helix and therefore shows only an overall preference for proline residues at all positions. Recognition interfaces of WW domains and profilin resemble the SH3 surface.

(D) Region of the Mena EVH1 domain that may interact with C-terminal acidic residues from ActA-derived ligands. A highly electropositive region (blue) is found immediately adjacent to the C terminus of the bound core peptide. Potential path of the continuing peptide chain is indicated by magenta spheres. Figure was generated using GRASP, Molscript, and RASTER3D.

cross-react with the ligands of SH3 domains (Gertler et al., 1996; Niebuhr et al., 1997) (Figure 2C). Peptide binding specificity and register is conferred by critical nonproline residues that flank the proline-rich core. A phenylalanine that is N-terminal to the proline core is required for recognition by the Mena and WASP EVH1 domains (Figure 2C). The EVH1 structure reveals a corresponding pocket that specifically recognizes this Phe or other large hydrophobic residues (such as leucine, found in the human Robo sequence). Additionally, the highest-affinity EVH1 ligands contain acidic residues surrounding the core sequence (Figure 2B). Although such acidic residues are not included in the crystallized Mena EVH1–peptide complex, we postulate that these interact with several basic residues on the EVH1 surface, found flanking the proline-binding aromatic triad (Figure 4D).

There is also a relatively high degree of peptide ligand discrimination among individual EVH1 domains, such as those from Mena, WASP, and Homer. This specificity also involves critical residues that flank the proline-rich core (Figure 2C). Although the detailed basis of ligand specificity among EVH1 domains remains to be elucidated, the Mena EVH1 domain structure yields some clues. The Homer/Vesl domain exhibits the most distinct binding specificity. Among the domains examined, it is the only one that binds the motif TPPSPFR from the metabotropic glutamate receptor and the SH3-binding motif PPPVPPRR. Also, Homer is the only domain that does not bind the sequence DFPPPTDEEL from ActA with high affinity. Correspondingly, within the EVH1 family, the Homer sequence shows the highest divergence at key positions involved in peptide recognition. For example, the aromatic triad residue Tyr-16 is conserved in Mena, VASP, and WASP but is replaced by Ile in Homer (Figure 3C). Moreover, residues that are structurally adjacent to the aromatic triad show considerable variability and may contribute to ligand discrimination among individual EVH1 domains. The resulting sequence preferences may be what allow Homer to localize to distinct sites compared to Enabled/VASP/WASP family members.

EVH1 Domains Are Distinct Members of the PH Domain Superfamily

Despite extremely low sequence homology, the crystal structure of the EVH1 domain of Mena reveals an overall fold that closely resembles that of PH domains. In general, PH domains bind to acidic phospholipids and mediate protein localization to the plasma membrane (Rameh et al., 1997; Kavran et al., 1998). PTB domains are another class of peptide recognition modules that are structurally similar to PH domains (Zhou and Fesik, 1995; Zhou et al., 1996; Zhang et al., 1997; Li et al., 1998).

PH, PTB, and EVH1 domains form phylogenetically and functionally distinct branches of a diverse superfamily (Figure 5C). Despite their structural similarities, these domains bind their varied peptide or phospholipid

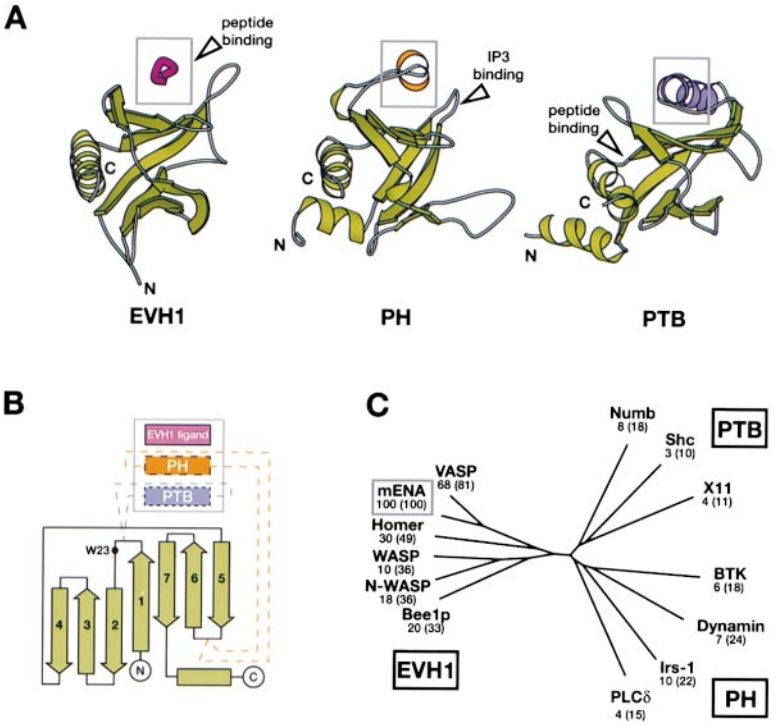

Figure 5. EVH1 Fold Is Similar to Pleckstrin Homology (PH) and Phosphotyrosine-Binding (PTB) Domain Folds

(A) Comparison of the Mena EVH1 domain with the PH domain from phospholipase C δ (Ferguson et al., 1995) and the PTB domain from dNumb (Li et al., 1998). The intermolecular peptide ligand (magenta) in the EVH1 complex structure is replaced by inserted intramolecular interactions in the PH (helical insert in orange) and PTB (helical insert in blue) domains. In PH domains, the inserted element occurs between the fifth and sixth β strands; in PTB domains, it occurs between the first and second β strands. EVH1 domains lack inserts at these sites. The ligand-binding sites of PH and PTB domains [PH, Inositol-(3,4,5) triphosphate; PTB, GPPY peptide] are highlighted by arrows and are distinct from the EVH1 peptide-binding site.

(B) Secondary structure diagram shows the common topology. PH and PTB domains, however, have the indicated insertions in the sequence.

(C) Dendrogram indicating sequence relationship of PH, PTB, and EVH1 branches of the PH fold superfamily. Percent sequence identity and similarity (in parentheses) to the Mena EVH1 domain are given below each protein. Alignments and trees were generated using the program Clustal X. Additional PH and PTB domains were used in the analysis but are not shown for clarity.

ligands using distinct binding sites distributed across the domain surface (Figure 5A). The PH topology may be a particularly robust and functionally plastic platform for binding a wide range of ligands. The PH fold appears to have been used for many distinct purposes throughout evolution, much as observed for the immunoglobulin superfamily (Cohen et al., 1995).

The distinct branches of the PH superfamily have intriguing structural differences that are intimately tied to functional differences. The most distinguishing feature of EVH1 domains is the lack of an additional segment of secondary structure found in both PH and PTB domains (Figures 5A and 5B). In PH and PTB domains, this extra segment adopts either a helix or loop conformation and packs at what is the peptide-binding site of the EVH1 domain. The absence of these segments in EVH1 domains may be what allows this site to serve as a peptide-binding platform. Peptide binding by the EVH1 domain may serve to complete the fold of the protein, as the intermolecular ligand interaction can be viewed as substituting for what is normally an intramolecular interaction in PH and PTB domains.

Peptide Binding and Membrane Association: Possible Mechanism for EVH1 Targeting to the Leading Edge

The structural similarity between EVH1 domains and PH domains is highly suggestive given that sites of dynamic actin remodeling are invariably plasma membrane associated. Moreover, the EVH1 domain of N-WASP is reported to interact with phosphatidyl inositol-4-phosphate (PIP) and phosphatidyl inositol-4,5-phosphate (PIP_2) (Miki et al., 1996).

These observations suggest that proper targeting of EVH1 domains could involve membrane association (Figure 6A). An auxiliary association with membranes could enhance the targeting specificity of EVH1 domains, explaining why EVH1 proteins localize to plasma membrane sites, as opposed to cytoplasmic sites that may bear related FPPPP motifs. For example, the signaling protein Shc is found to properly localize and function only if its PTB domain can interact with both phospholipid and peptide ligands (Ravichandran et al., 1997).

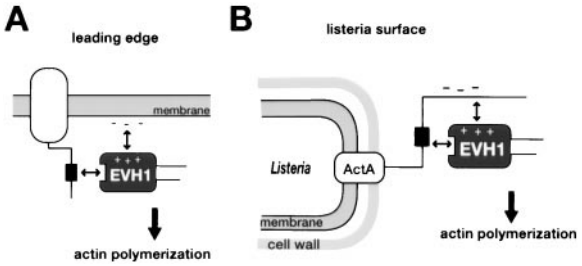

Figure 6. Possible Mechanism for EVH1 Domain Targeting of Actin Assembly

(A) EVH1 proteins may recognize proline-rich peptides (solid rectangle) in an acidic phospholipid context to selectively localize to leading edge membrane sites.

(B) Pathogens such as *Listeria monocytogenes* may use peptide ligand sequences that emulate the combination of interactions described in (A). The ActA sequences have a high density of negatively charged residues immediately C-terminal to the peptide's proline-rich core peptide sequence. Such ligands have higher affinity than host-derived ligands and may constitutively recruit EVH1 domain proteins in a nonmembrane context (e.g., outside of the cell wall of the gram-positive bacteria).

EVH1 domain interactions with phospholipids would also allow for regulation by phosphoinositide kinases and phosphatases, enzymes known to play a role in motility (Zigmond, 1996).

Membrane association, which might involve the highly basic surface path found on the EVH1 domain (Figure 4D), could also explain why the motifs found in the *Listeria* ActA protein are of significantly higher affinity than host-binding motifs. ActA is a pathogenic protein that must promote constitutive actin polymerization, in contrast to the regulated polymerization promoted by host factors. Moreover, ActA must perform this task in the absence of both the host and pathogen membranes (the *Listeria* membrane is occluded by its external cell wall). Thus, the higher affinity motifs in ActA may have evolved to allow constitutive EVH1 recruitment in a nonmembranous context. It is striking that the major element responsible for the high affinity of ActA motifs (DFPPPTDEEL) is a stretch of acidic residues that flank the core FPPPP motif (Figure 2B). This high negative charge density may emulate the overall electrostatic properties involved in EVH1 recognition of peptide in a phospholipid membrane context (Figure 6B).

Conclusions

Our studies show that the EVH1 domain uses a conformation-based mechanism of peptide recognition, primarily recognizing the PPII helix adopted by the proline-rich core. This mechanism differs from that of SH3 domains and other previously characterized proline-binding modules and explains why EVH1 domains have a preference for a high density of proline residues rather than an absolute requirement for prolines at specific positions. We also find that the EVH1 domains are structurally homologous to PH domains. Thus, the PH superfamily fold appears to be an extremely plastic binding scaffold. The structural homology to PH domains and the previous observation that some EVH1 domains can interact with phospholipids suggest that EVH1 domains may target actin assembly to leading edge sites by coordinately interacting with peptide motifs and membrane phospholipids. Such dual interactions could greatly enhance the regulation and spatial precision of EVH1 protein recruitment and would be very useful in mediating coordinated cell movements. Pathogens such as *Listeria* appear to have evolved high-affinity binding motifs that allow for constitutive EVH1 domain recruitment, independent of any membrane interactions. Understanding the molecular basis of these early events in cell movement may allow for the development of new therapeutic agents directed against diseases involving motility, including listereosis, inflammation, and metastatic cancer.

Experimental Procedures

Protein Expression and Purification

The DNA sequence corresponding to residues 1 to 112 of Mena (the minimal fragment sufficient for ActA peptide binding) was amplified by PCR from a mouse brain cDNA library and cloned into the T7 expression vector pBH4, which contains an N-terminal 6× His tag and a TEV protease cleavage site. Mena 1–112 protein was expressed in *E. coli* strain BL21(DE3). Six liters of cells were grown to $OD_{600} = 1$, induced with 1 mM IPTG, and grown for an additional 3 hr. Cells were harvested and lysed by sonication in 100 ml of 150 mM Na-PO_4 (pH 7.5), 10 mM imidazole. Protein was purified on 10 ml Ni-NTA superflow resin (Qiagen) by elution with a 20–150 mM imidazole step gradient and dialyzed against 50 mM HEPES, 0.3 M NaCl, 5 mM DTT, 5 mM EDTA. The 6× His tag was removed by cleavage with recombinant TEV protease, as monitored by SDS-PAGE. The cleavage reaction mixture was repassaged over fresh Ni-NTA resin to remove the cleaved 6× His tag and TEV protease (itself containing a 6× His tag). Final purification was achieved by chromatography on a 20 ml Source S column (Pharmacia), eluting with a gradient of 20–500 mM NaCl in 25 mM HEPES (pH 7.5). Protein was dialysed against 10 mM HEPES (pH 7.0), 20 mM NaCl, 5 mM DTT and concentrated to 30 mg ml^{-1} by ultrafiltration (Amicon). Purity and identity of the protein was confirmed by SDS-PAGE and mass spectrometry. Peptides were synthesized manually or on an ABI 431 peptide synthesizer by Fmoc chemistry, purified by reversed-phase HPLC, and analyzed by mass spectrometry.

Selenomethionine (SeMet)-labeled Mena 1–112 protein was produced by growth in minimal media supplemented with selenomethionine as previously described (Van Duyne et al., 1993). The purification was identical to the native protein except that all buffers were purged to prevent selenium oxidation. Labeling was confirmed by mass spectrometry.

Crystallographic Methods

Crystals were obtained by sitting drop vapor diffusion. Five microliters of 15 mg ml^{-1} SeMet Mena 1–112 and 6 mM Ac-FPPPPT-$CONH_2$ were mixed with an equal volume of well solution containing 60% saturated $(NH_4)_2HPO_4$, 0.1 M HEPES (pH 7.5) at 20°C. Within 2 days, a shower of microneedles formed. However, in approximately 20% of the drops, clusters of a larger plate crystal form appeared within the needles shower. Formation of plates could also be induced by microseeding. Over 2–4 weeks, the initial microneedles completely converted into the plate crystal form. Average crystal dimensions were 15 × 50 × 500 μ. No diffraction quality crystals were obtained with any of the longer length ActA-derived peptides utilized in crystallization trials. Prior to data collection, crystals were transferred to cryoprotectant (mother liquor + 20% glycerol) and flash frozen in liquid nitrogen.

Crystals grew in space group $C222_1$ (a = 33.6 Å, b = 62.6 Å, c = 94.3 Å) with one EVH1 monomer per asymmetric unit. MAD diffraction data was collected at four wavelengths at beamline 5.0.2 at the Advanced Light Source (ALS) at Lawrence Berkeley Laboratories using an ADSC Quantum-4 CCD detector. All data were collected on a single selenomethionine-substituted protein crystal. A fluorescence scan of the crystal was taken to optimize data collection and to calculate anomalous scattering coefficients. Diffraction data was processed and scaled using the HKL software package (Otwinowski and Minor, 1997).

Using the data sets from wavelengths 2, 3, and 4 (Table 1), three of the four selenium sites were identified by the Patterson search methods in the program SOLVE (Terwilliger and Berendzen, 1996). These sites were further refined using the program SHARP (De La Fortelle and Bricogne, 1997), inputing the anomalous scattering coefficients from the experimental fluorescence scan. The MAD phases were further improved with solvent flipping, using the program SOLOMON (Collaborative Computational Project, 1994).

Model Building and Refinement

The initial model was built using the program O (Jones et al., 1991). The experimental map was readily traceable and allowed for the construction of a model of residues 2–112 of Mena. Residues 1–5 of the peptide were also evident in the experimental map but were not included until later stages in the refinement. The model was refined against the MAD data using the program CNS (version 0.4) (Brünger et al., 1998) with alternate cycles of rebuilding, positional refinement, and restrained B factor refinement. All diffraction data was used throughout, except a 10% test set for calculation of the free R factor.

Far Western Protein Interaction Assays

Putative EVH1 peptide ligands were generated as fusions to glutathione S-transferase (GST) by ligating the appropriate oligonucleotides

into the BamHI and EcoRI restriction sites of plasmid pGEX4T-1 (Pharmacia). GST fusion proteins were expressed in *E. coli* strain TG1 by growing a 1 l culture to $OD_{600} = 1$ and inducing with 1 mM IPTG. After 3 hr of further growth, cells were harvested, lysed by sonication, and the fusion protein purified on 100 μl of glutathione agarose resin (Sigma). After washing with 25 mM Tris HCl (pH 7.5), 150 mM NaCl, 1 mM EDTA, the resin was boiled in SDS-PAGE loading buffer and an aliquot electrophoresed on a 10%–20% SDS-PAGE gel. Fusion protein bands were transferred to nitrocellulose by electroblotting and blocked for 1 hr at 4°C in 50 mM Tris (pH 7.5), 150 mM NaCl, 0.1% TWEEN (TBST) with 1% nonfat milk and 1% bovine serum albumin.

Biotinylated EVH1 and control SH3 domain probes were produced as fusions to a naturally biotinylated *E. coli* protein using the PINPOINT system (Promega). The DNA fragments encoding the desired protein segments (Mena 1–112, hWASP 1–170, dHomer 1–112, mSrc 87–142) were amplified from human, mouse, or *Drosophila* cDNA libraries by PCR and ligated into the BamHI and NotI sites of the plasmid PINPOINT Xa-3. The PINPOINT fusion proteins were expressed as described for the GST fusion proteins. The sonicated and centrifuged lysate was used directly, after estimating fusion protein concentration by SDS-PAGE.

To detect binding, blocked nitrocellulose filters bearing the putative ligand fusion proteins were incubated at 4°C for 45 min with the appropriate biotinylated EVH1 domain probe at a concentration of ~0.25 mg/ml in 5 ml of the above blocking buffer. Filters were washed three times with ~100 ml TBST, incubated for 10 min with four units of streptavidin-conjugated horseradish peroxidase (Boehringer Mannheim) in 20 ml TBS (TBST without TWEEN), washed three times in ~100 ml TBST, and the bands visualized by enhanced chemiluminescence.

Fluorescence Peptide Binding Assay

Fluorescence titration was used to measure peptide binding affinities to the Mena EVH1 domain. Increasing amounts of peptide, from a 50 mM peptide stock, were titrated into a stirred cuvette with a 1.25 ml solution of 0.5 μM Mena (residues 1–112) in 20 mM HEPES (pH 7.5), 20 mM NaCl at 20°C. The intrinsic fluorescence (excitation 280 nm, emission 330 nm) of the Mena EVH1 domain over the course of the titration was monitored with a PTI fluorometer. At saturation, peptide binding resulted in an ~1.2-fold increase in fluorescence emission intensity. Fluorescence signal at each point was averaged for at least 30 s. For each experiment, at least 12 concentration points were measured. Intensity measurements were corrected for dilution and the resulting binding isotherm fit using the program proFit (Quantum Soft) to determine dissociation constants (K_D). The standard deviation was estimated at ±10%, based on replicate experiments. Data fit to a 1:1 domain–peptide stoichiometry, which was independently confirmed by analytical ultracentrifugation, light scattering (K. E. P., unpublished data), and the crystal structure.

Acknowledgments

We thank S. Blanchard and D. Halpin for contributions at the inception of this project; B. Ruivivar for her dedication; C. Turck and T. Earnest of ALS (Department of Energy, Lawrence Berkeley Laboratory) and members of the UCSF Macromolecular Structure Group for assistance; M. Caterina, D. Bredt, and H. Ingraham for providing mRNA; and C. Bargmann, H. Bourne, D. Julius, D. Mullins, J. Theriot, J. Weissman, K. Yamamoto, T. Yu, and members of the Lim lab for comments and discussion. This work was supported by grants to W. A. L. from the National Institutes of Health, the HHMI Research Resources Program, the Burroughs Wellcome Young Investigator Program, the Searle Scholars Program, and the Packard Foundation. K. E. P. is a Cancer Research Institute Postdoctoral Fellow. Coordinates will be deposited in the Protein Data Bank.

Received March 18, 1999; revised April 15, 1999.

References

Beckerle, M.C. (1998). Spatial control of actin filament assembly: lessons from *Listeria*. Cell *95*, 741–748.

Bottomley, M.J., Salim, K., and Panayotou, G. (1998). Phospholipid-binding protein domains. Biochim. Biophys. Acta *1436*, 165–183.

Brakeman, P.R., Lanahan, A.A., O'Brien, R., Roche, K., Barnes, C.A., Huganir, R.L., and Worley, P.F. (1997). Homer: a protein that selectively binds metabotropic glutamate receptors. Nature *386*, 284–288.

Brünger, A.T., Adams, P.D., Clore, G.M., DeLano, W.L., Gros, P., Grosse-Kunstleve, R.W., Jiang, J.-S., Kuszewski, J., Nilges, M., Pannu, N.S., et al. (1998). Crystallography and NMR system: a new software suite for macromolecular structure determination. Acta Crystallogr. D *54*, 905–921.

Chakraborty, T., Ebel, F., Domann, E., Niebuhr, K., Gerstel, B., Pistor, S., Temm-Grove, C.J., Jockusch, B.M., Reinhard, M., Walter, U., et al. (1995). A focal adhesion factor directly linking intracellularly motile Listeria monocytogenes and Listeria ivanovii to the actin-based cytoskeleton of mammalian cells. EMBO J. *14*, 1314–1321.

Cohen, G.B., Ren, R., and Baltimore, D. (1995). Modular binding domains in signal transduction proteins. Cell *80*, 237–248.

Collaborative Computational Project (1994). The CCP4 suite: programs for protein crystallography. Acta Crystallogr. D *50*, 760–763.

De La Fortelle, E., and Bricogne, G. (1997). Maximum-likelihood heavy-atom parameter refinement for muliple isomorphous replacement and multiwavelength anomalous diffraction methods. Methods Enzymol. *276*, 472–494.

Feng, S., Chen, J.K., Yu, H., Simon, J.A., and Schreiber, S.L. (1994). Two binding orientations for peptides to the Src SH3 domain: development of a general model for SH3-ligand interactions. Science *266*, 1241–1247.

Ferguson, K.M., Lemmon, M.A., Schlessinger, J., and Sigler, P.B. (1995). Structure of the high affinity complex of inositol trisphosphate with a phospholipase C pleckstrin homology domain. Cell *83*, 1037–1046.

Finan, P.M., Soames, C.J., Wilson, L., Nelson, D.L., Stewart, D.M., Truong, O., Hsuan, J.J., and Kellie, S. (1996). Identification of regions of the Wiskott-Aldrich syndrome protein responsible for association with selected Src homology 3 domains. J. Biol. Chem. *271*, 26291–26295.

Gertler, F.B., Niebuhr, K., Reinhard, M., Wehland, J., and Soriano, P. (1996). Mena, a relative of VASP and Drosophila Enabled, is implicated in the control of microfilament dynamics. Cell *87*, 227–239.

Haslam, R.J., Koide, H.B., and Hemmings, B.A. (1993). Pleckstrin domain homology. Nature *363*, 309–310.

Huttelmaier, S., Mayboroda, O., Harbeck, B., Jarchau, T., Jockusch, B.M., and Rudiger, M. (1998). The interaction of the cell-contact proteins VASP and vinculin is regulated by phosphatidylinositol-4,5-bisphosphate. Curr. Biol. *8*, 479–488.

Jones, T.A., Zou, J.-Y., and Cowan, S.W. (1991). Improved methods for building models in electron density maps and the location of errors in these models. Acta Crystallogr. A *47*, 110–119.

Kato, A., Ozawa, F., Saitoh, Y., Hirai, K., and Inokuchi, K. (1997). vesl, a gene encoding VASP/Ena family related protein, is upregulated during seizure, long-term potentiation and synaptogenesis. FEBS Lett. *412*, 183–189.

Kavran, J.M., Klein, D.E., Lee, A., Falasca, M., Isakoff, S.J., Skolnik, E.Y., and Lemmon, M.A. (1998). Specificity and promiscuity in phosphoinositide binding by pleckstrin homology domains. J. Biol. Chem. *273*, 30497–30508.

Kidd, T., Brose, K., Mitchell, K.J., Fetter, R.D., Tessier-Lavigne, M., Goodman, C.S., and Tear, G. (1998). Roundabout controls axon crossing of the CNS midline and defines a novel subfamily of evolutionarily conserved guidance receptors. Cell *92*, 205–215.

Kuriyan, J., and Cowburn, D. (1997). Modular peptide recognition domains in eukaryotic signaling. Annu. Rev. Biophys. Biomol. Struct. *26*, 259–288.

Lanier, L.M., Gates, M.A., Witke, W., Menzies, A.S., Wehman, A.M., Macklis, J.D., Kwiatkowski, D., Soriano, P., and Gertler, F.B. (1999). Mena is required for neurulation and commissure formation. Neuron *22*, 313–325.

Laurent, V., Loisel, T.P., Harbeck, B., Wehman, A., Gröbe, L., Jockusch, B.M., Wehland, J., Gertler, F.B., and Carlier, M.F. (1999). Role of proteins of the Ena/VASP family in actin-based motility of Listeria monocytogenes. J. Cell Biol. *144*, 1245–1258.

Li, R. (1997). Bee1, a yeast protein with homology to Wiscott-Aldrich syndrome protein, is critical for the assembly of cortical actin cytoskeleton. J. Cell Biol. *136*, 649–658.

Li, S.C., Zwahlen, C., Vincent, S.J., McGlade, C.J., Kay, L.E., Pawson, T., and Forman-Kay, J.D. (1998). Structure of a Numb PTB domain-peptide complex suggests a basis for diverse binding specificity. Nat. Struct. Biol. *5*, 1075–1083.

Lim, W.A., Richards, F.M., and Fox, R.O. (1994). Structural determinants of peptide-binding orientation and of sequence specificity in SH3 domains. Nature *372*, 375–379.

Machesky, L.M. (1997). Cell motility: complex dynamics at the leading edge. Curr. Biol. *7*, R164–R167.

Machesky, L.M., and Insall, R.H. (1998). Scar1 and the related Wiskott-Aldrich syndrome protein, WASP, regulate the actin cytoskeleton through the Arp2/3 complex. Curr. Biol. *31*, 1347–1356.

Macias, M.J., Musacchio, A., Ponstingl, H., Nilges, M., Saraste, M., and Oschkinat, H. (1994). Structure of the pleckstrin homology domain from beta-spectrin. Nature *369*, 675–677.

Macias, M.J., Hyvonen, M., Baraldi, E., Schultz, J., Sudol, M., Saraste, M., and Oschkinat, H. (1996). Structure of the WW domain of a kinase-associated protein complexed with a proline-rich peptide. Nature *382*, 646–649.

Mahoney, N.M., Janmey, P.A., and Almo, S.C. (1997). Structure of the profilin-poly-L-proline complex involved in morphogenesis and cytoskeletal regulation. Nat. Struct. Biol. *4*, 953–960.

Mayer, B.J., Ren, R., Clark, K.L., and Baltimore, D. (1993). A putative modular domain present in diverse signaling proteins. Cell *73*, 629–630.

Miki, H., Miura, K., and Takenawa, T. (1996). N-WASP, a novel actin-depolymerizing protein, regulates the cortical cytoskeletal rearrangement in a PIP2-dependent manner downstream of tyrosine kinases. EMBO J. *15*, 5326–5335.

Mitchison, T.J., and Cramer, L.P. (1996). Actin-based cell motility and cell locomotion. Cell *84*, 371–379.

Nguyen, J.T., Turck, C.W., Cohen, F.E., Zuckermann, R.N., and Lim, W.A. (1998). Exploiting the basis of proline recognition by SH3 and WW domains: design of N-substituted inhibitors. Science *282*, 2088–2092.

Niebuhr, K., Ebel, F., Frank, R., Reinhard, M., Domann, E., Carl, U.D., Walter, U., Gertler, F.B., Wehland, J., and Chakraborty, T. (1997). A novel proline-rich motif present in ActA of Listeria monocytogenes and cytoskeletal proteins is the ligand for the EVH1 domain, a protein module present in the Ena/VASP family. EMBO J. *16*, 5433–5444.

Otwinowski, Z., and Minor, W. (1997). Processing of X-ray diffraction data collected in oscillation mode. Methods Enzymol. *276*, 307–326.

Pollard, T.D. (1995). Actin cytoskeleton. Missing link for intracellular bacterial motility? Curr. Biol. *5*, 837–840.

Ponting, C.P., and Phillips, C. (1997). Identification of homer as a homologue of the Wiskott-Aldrich syndrome protein suggests a receptor-binding function for WH1 domains. J. Mol. Med. *75*, 769–771.

Rameh, L.E., Arvidsson, A., Carraway, K.L., 3rd, Couvillon, A.D., Rathbun, G., Crompton, A., VanRenterghem, B., Czech, M.P., Ravichandran, K.S., Burakoff, S.J., et al. (1997). A comparative analysis of the phosphoinositide binding specificity of pleckstrin homology domains. J. Biol. Chem. *272*, 22059–22066.

Ravichandran, K.S., Zhou, M.M., Pratt, J.C., Harlan, J.E., Walk, S.F., Fesik, S.W., and Burakoff, S.J. (1997). Evidence for a requirement for both phospholipid and phosphotyrosine binding via the Shc phosphotyrosine-binding domain in vivo. Mol. Cell. Biol. *17*, 5540–5549.

Reinhard, M., Giehl, K., Abel, K., Haffner, C., Jarchau, T., Hoppe, V., Jockusch, B.M., and Walter, U. (1995). The proline-rich focal adhesion and microfilament protein VASP is a ligand for profilins. EMBO J. *14*, 1583–1589.

Smith, G.A., Theriot, J.A., and Portnoy, D.A. (1996). The tandem repeat domain in the Listeria monocytogenes ActA protein controls the rate of actin-based motility, the percentage of moving bacteria, and the localization of vasodilator-stimulated phosphoprotein and profilin. J. Cell Biol. *135*, 647–660.

Southwick, F.S., and Purich, D.L. (1994). Arrest of Listeria movement in host cells by a bacterial ActA analogue: implications for actin-based motility. Proc. Natl. Acad. Sci. USA *91*, 5168–5172.

Symons, M., Derry, J.M., Karlak, B., Jiang, S., Lemahieu, V., McCormick, F., Francke, U., and Abo, A. (1996). Wiskott-Aldrich syndrome protein, a novel effector for the GTPase CDC42Hs, is implicated in actin polymerization. Cell *84*, 723–734.

Terwilliger, T.C., and Berendzen, J. (1996). Correlated phasing of multiple isomorphous replacement data. Acta Crystallogr. D *52*, 749–757.

Theriot, J.A., Rosenblatt, J., Portnoy, D.A., Goldschmidt-Clermont, P.J., and Mitchison, T.J. (1994). Involvement of profilin in the actin-based motility of L. monocytogenes in cells and in cell-free extracts. Cell *76*, 505–517.

Tilney, L.G., and Portnoy, D.A. (1989). Actin filaments and the growth, movement, and spread of the intracellular bacterial parasite, Listeria monocytogenes. J. Cell Biol. *109*, 1597–1608.

Tu, J.C., Xiao, B., Yuan, J.P., Lanahan, A.A., Leoffert, K., Li, M., Linden, D.J., and Worley, P.F. (1998). Homer binds a novel proline-rich motif and links group 1 metabotropic glutamate receptors with IP3 receptors. Neuron *21*, 717–726.

Van Duyne, G.D., Standaert, R.F., Karplus, P.A., Schreiber, S.L., and Clardy, J. (1993). Atomic structures of the human immunophilin FKBP-12 complexes with FK506 and rapamycin. J. Mol. Biol. *229*, 105–124.

Yoon, H.S., Hajduk, P.J., Petros, A.M., Olejniczak, E.T., Meadows, R.P., and Fesik, S.W. (1994). Solution structure of a pleckstrin-homology domain. Nature *369*, 672–675.

Yu, H., Chen, J.K., Feng, S., Dalgarno, D.C., Brauer, A.W., and Schreiber, S.L. (1994). Structural basis for the binding of proline-rich peptides to SH3 domains. Cell *76*, 933–945.

Zallen, J.A., Yi, B.A., and Bargmann, C.I. (1998). The conserved immunoglobulin superfamily member SAX-3/Robo directs multiple aspects of axon guidance in *C. elegans*. Cell *92*, 217–227.

Zhang, Z., Lee, C.H., Mandiyan, V., Borg, J.P., Margolis, B., Schlessinger, J., and Kuriyan, J. (1997). Sequence-specific recognition of the internalization motif of the Alzheimer's amyloid precursor protein by the X11 PTB domain. EMBO J. *16*, 6141–6150.

Zhou, M.M., and Fesik, S.W. (1995). Structure and function of the phosphotyrosine binding (PTB) domain. Prog. Biophys. Mol. Biol. *64*, 221–235.

Zhou, M.M., Huang, B., Olejniczak, E.T., Meadows, R.P., Shuker, S.B., Miyazaki, M., Trub, T., Shoelson, S.E., and Fesik, S.W. (1996). Structural basis for IL-4 receptor phosphopeptide recognition by the IRS-1 PTB domain. Nat. Struct. Biol. *3*, 388–393.

Zigmond, S.H. (1996). Signal transduction and actin filament organization. Curr. Opin. Cell Biol. *8*, 66–73.

Protein Data Bank ID Code

The Mena EVH1 complex coordinates reported in this paper have been deposited in the Protein Data Bank under ID code 1evh.